Numerical and Theoretical Investigations of Heat Transfer Characteristics of the Phase Change Process of Wick Heat Pipe Evacuated Tube Solar Collector

[1]Sandar Hlaing, [2]Mi Sandar Mon
[1]Ph.D Candidate, Department of Mechanical Engineering, Yangon Technological University, Yangon, Myanmar
[2]Professor and Head, Department of Mechanical Engineering, Yangon Technological University, Yangon, Myanmar
Email - [1]sandarhlaing516@gmail.com, [2]msdmon@gmail.com

Abstract: *Solar energy is one of the renewable energies to be used in various applications. Myanmar is located near the equator where solar energy is abundant. So, in this research, water heating systems are supplied by using solar insolation and wick heat pipe evacuated tube solar collector (ETC). The design location to investigate the total monthly solar insolation is based on Insein, Yangon Technological University(YTU) location with North Latitude 16.87^o, East Longitude 96.11^o and elevation above sea level 20m. Heat transfer working fluid, water (0.006L) was used within the heat pipe. This research emphasizes on the numerical and theoretical investigations of heat transfer characteristics of a wick heat pipe(ETC) with the variation of inclination angle effect. The capillary effect is assisted although the gravity effect is not considered to determine the thermal behaviour. Numerical simulations were be widely used to investigate the heat transfer characteristics with velocity distribution in a wick heat pipe. Moreover, theoretical calculations were investigated by using three different techniques.*

Key Words: *Evacuated Tube, Inclination Angle, Numerical and Theoretical Investigations, Wick Heat Pipe.*

1. INTRODUCTION:

Solar water heating systems by using solar collector have significant potential to reduce environmental pollution arising from the use of fossil fuels. Heat pipe(ETC) is higher performance efficiency and larger amount of heat energy output than other collectors. Hossein Abdi investigated water outlet temperature, efficiency and useful heat gain with the variable mass flow rate and number of heat pipe by using heat pipe evacuated tube solar collector according to the theoretical and experimental findings [1]. This research showed that the water outlet temperature improved by decreasing mass flow rate and increasing number of heat pipe. Moreover, Siva Kumar investigated water outlet temperature and efficiency of heat pipe(ETC) by theoretical and experimental techniques [2]. This investigation obtained that the maximum water outlet temperature at the highest solar radiation. Isam has described wall diameter, heat flux, and porosity variation inside heat pipe in detail using numerical simulation [3]. Wall diameter shows that the conduction heat transfer through wall does not change much with wall thickness. Heat flux clearly demonstrate that the maximum heat transfer and so the wall temperature occur with maximum power. Porosity means that the heat pipe with lower porosity is better. Moreover, Shoeib Mahjoub in 2008 carried out tests to analyse the numerical simulation of a conventional electronic wick heat pipe and performance study by using FLUENT software [4]. Rakesh analysed numerical investigations of two phase flow in a wick heat pipe [5]. According to this result, liquid and vapor flow processes were examined that at wick and vapor core regions. Nagham Ismail examined condenser outlet temperature, water outlet temperature and efficiency of wick heat pipe flat plate collector, all-glass(ETC) and heat pipe(ETC) by theoretical(NTU) method and experimental conditions [6]. This observe showed that heat pipe(ETC) is larger amount of heat energy output than other collectors.

The working principle of a wick heat pipe (ETC) is shown in Figure 1. A small quantity of liquid is placed in a wick. The bottom of the wick heat pipe(ETC) evaporator section is heated, this causing that the vapor flows from the liquid wick region to the vapor core region. After that, the vapor rises to the top of the condensation section where it is cooled and condensed into liquid. The copper heat pipe transmits heat to its tip which is plugged into the collector's heat transfer manifold. As water runs through the manifold heat is transferred from the copper heat pipe to the water. Then the liquid flows downwards by capillary effect to the liquid wick region. This entire cycle repeats in wick heat pipe(ETC) again and again. In this paper, condenser outlet temperature, phase change process and velocity distribution were determined by numerical investigations. Moreover, in this research, wick effect is more considered within a heat pipe to determine the heat transfer characteristics for horizontal and low incline angles. After that, these results were compared with three different theoretical techniques of wick heat pipe (ETC) depend on the effect of collector inclination angles.

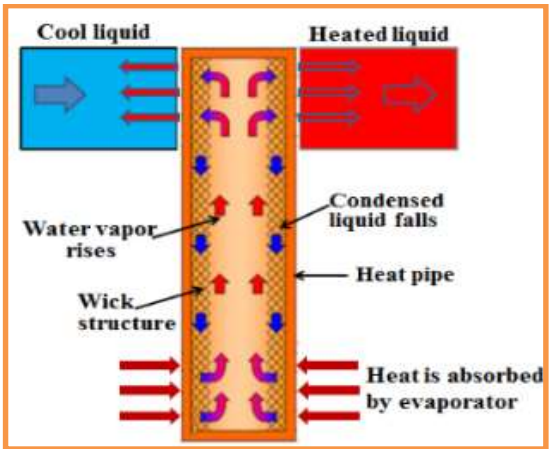

Fig. 1 Working Principle of a Wick Heat Pipe(ETC)

2. SOLAR RADIATION:

2.1. Solar Radiation Calculation

In this paper, the design location is Insein, Yangon Technological University(YTU). The design month is considered from January to December 2017 at 12:00 noon.

North Latitude = 21.98º N

East Longitude = 96.1ºE

I_o, solar constant value = 1373W/m^2

Elevation above sea level = 20 m

Local standard time of meridian for Yangon is 97.5ºE

2.1.1 Essential Solar Angles for Solar Radiation

Solar declination angle,

$$\delta = 23.45\sin\left[\frac{360}{365}(284+n)\right] \quad (1)$$

Solar zenith angle,

$$\theta_z = \cos^{-1}[\sin\lambda\ \sin\delta + \cos\lambda\ \cos\delta\ \cos\omega] \quad (2)$$

Solar hour angle,

$$\omega = \frac{360}{\tau_{day}}\ t \quad (3)$$

2.1.2 Monthly Beam, Diffuse, Hemispherical, Effective and Total Solar Insolation

Beam radiation,

$$I_b = I_{0,eff}\left[a_0 + a_1\exp\left(-\frac{k}{\cos\theta_z}\right)\right] \quad (4)$$

Diffuse radiation,

$$I_d = [0.2710\, I_{0,eff} - 0.2939\, I_b]\cos\theta_z \quad (5)$$

Hemispherical radiation,

$$I_h = I_b\cos\theta_z + I_d \quad (6)$$

Effective solar radiation,

$$I_{0,eff} = I_0[1 + 0.033\cos(\frac{360n}{365.25})] \quad (7)$$

Total solar insolation,

$$I = I_b\cos\theta + I_d(1+\cos\beta)/2 + I_h\,\rho_{ground}(1-\cos\beta)/2 \quad (8)$$

3. METHODOLOGY:

3.1. Numerical Modeling

In the numerical computation, finite volume method is based with SIMPLE algorithm and wick effect to solve the problem of heat transfer process, velocity and pressure coupling. The phase change occurs near the liquid-vapor interface between liquid-wick and vapor core regions. The liquid flow in the wick is due to the capillary action and is usually modelled as flow through porous medium. Water liquid and vapor flows are considered as transient, incompressible and laminar flow. All thermo physical properties are assumed to be constant. In this study, continuity, momentum and energy source terms are not employed to the FLUENT package. Moreover, body force terms such as gravity are considered to be negligible.

3.2. Governing Equations

The continuity and momentum equations for vapor and liquid-wick regions in the CFD model are:
Continuity equation for vapor region,

$$\frac{\partial \rho}{\partial t} + \rho \, \nabla . \vec{V} = 0 \tag{9}$$

Continuity equation for liquid-wick region,

$$\varepsilon \frac{\partial \rho}{\partial t} + \rho \, \nabla . \vec{V} = 0 \tag{10}$$

Momentum equation for vapor region,

$$\frac{\partial}{\partial t}(\rho \, u) + \nabla . (\rho \, \vec{V} \, u) = -\frac{\partial P}{\partial x} + \nabla . (\mu \, \nabla u) \tag{11}$$

$$\frac{\partial}{\partial t}(\rho \, v) + \nabla . (\rho \, \vec{V} \, v) = -\frac{\partial P}{\partial y} + \nabla . (\mu \, \nabla v) \tag{12}$$

Momentum equation for liquid-wick region,

$$\frac{\partial}{\partial t}(\rho \, u) + \nabla . (\rho \, \vec{V} \, u) = -\frac{\partial \varepsilon \, P}{\partial x} + \nabla . (\mu \, \nabla u) - \frac{\mu \varepsilon}{K} u - \frac{C_E}{K^{0.5}} \rho \left| \vec{V} \right| u \tag{13}$$

$$\frac{\partial}{\partial t}(\rho \, v) + \nabla . (\rho \, \vec{V} \, v) = -\frac{\partial \varepsilon \, P}{\partial y} + \nabla . (\mu \, \nabla v) - \frac{\mu \varepsilon}{K} v - \frac{C_E}{K^{0.5}} \rho \left| \vec{V} \right| v \tag{14}$$

Energy equation for heat pipe wall, liquid-wick and vapor regions

$$\frac{\partial (\rho \, C)_m T}{\partial t} + \nabla . \left[(\rho \, C)_L \, \vec{V} \, T_L \right] = \nabla . (k_{eff} \nabla T) \tag{15}$$

In this equation (15) $(\rho C)_m$ assumes different values in the heat pipe wall, liquid-wick and vapor regions: For heat pipe wall $(\rho C)_m = (\rho C)_s$, for liquid − wick $(\rho C)_m = (1-\varepsilon)(\rho C)_w + \varepsilon(\rho C)_L$ and for vapor region $(\rho C)_m = (\rho C)_v$ .The second term of Eq.(15) is neglected for the heat pipe wall region. k_{eff} is the effective thermal conductivity of the region of interest such as heat pipe wall and liquid-wick combination. k_{eff} is determined by the following Eq.(16)

In this equation, the porosity of the wick while using the water liquid is calculated by the following equation.

$$\varepsilon = 1 - \frac{1.05\pi}{4} N d_w \tag{17}$$

$$\frac{k_{eff}}{k_L} = \left[\frac{(k_L + k_w) - (1-\varepsilon)(k_L - k_w)}{(k_L + k_w) + (1-\varepsilon)(k_L - k_w)} \right] \tag{16}$$

3.3. Model Geometry

A two-dimensional double precision transient screen-mesh wick heat pipe model by using rectangular coordinate system was developed to simulate the two-phase flow and heat transfer phenomena in a wick heat pipe. The evaporator and condenser sections of the wick heat pipe model are 1.34m and 0.06m in length, making the adiabatic section 0.3m long. The outer and inner diameters are 0.008m and 0.0066m, respectively. The thickness of the wick is 0.0002286m. The combination of solid and fluid regions contains 136000 Quad cells. The grid generation of wick heat pipe(ETC) is shown in Figure 2.

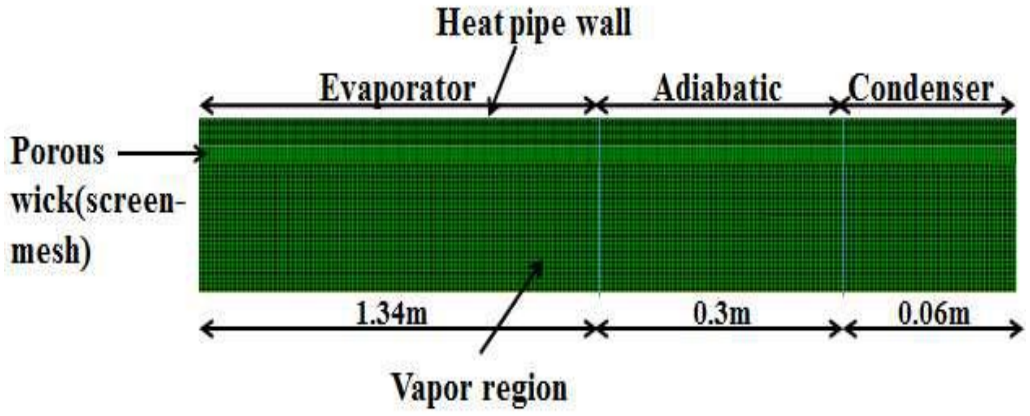

Fig. 2 2-D Geometry and Grid Generation of Wick Heat Pipe(ETC) in Gambit

3.4. Boundary Condition and Initial Condition

A non-slip boundary condition was imposed at the inner walls of the heat pipe. The constant solar heat fluxes were defined at the wall boundaries of the evaporator section for all inclination angles. A zero heat flux is defined as boundary condition on the adiabatic section. Moreover, adiabatic conditions are provided at the top and bottom wall of the heat pipe. The condenser section was cooled as a result of heat released when vapor condenses. Thus, negative sign constant heat flux values were defined as boundary condition on the condenser's wall according to the energy balance theory. Between the liquid-wick and vapor regions are regarded mass flow inlet and outlet at evaporator and condenser zones. And then, the adiabatic zone is assigned interface boundary condition.

In the initial condition, the filling ratio, which means the ratio of the initial liquid volume to the total volume of the evaporation section, is set to 30% which is 6mL as depicted. Also, the initial temperature of the liquid-wick and vapor regions is set to 303K. This temperature will lead to a steady state quickly because the saturation temperature is 322K at one atmosphere pressure.

A transient simulation with a time step of 0.05 s is carried out to model the dynamic behavior of the two phase flow. The simulation operating condition took the temperature more than about 3months for (35°, 25°, 15°, 15°, 0°, 0°, 0°, 10°, 15°, 20°, 35°, 40°) inclination angles from January to December depend on YTU location to reach a steady state using the computer with Intel Core i3 CPU, 32 GB RAM and 32 bit operating system.

3.5. Theoretical Modeling

According to this wick heat pipe(ETC) theoretical modeling, condenser outlet temperature of wick heat pipe(ETC) has been investigated by using three different tests such as Nagham Ismail's NTU method(method-1), Siva Kumar's empirical formula(method-2) and Islamic Azad's simple heat transfer formula(method-3). In these methods, the overall heat loss coefficient between the collector and ambient after that between the manifold casing and ambient are assumed to be negligible. In method-1, conduction and convection heat transfer coefficient were considered between condenser and manifold however method-2 determined only the convection heat transfer coefficient. Moreover, method-3 investigated only the conduction heat transfer coefficient. In table 3.1, shows three different methods with thermal resistances. However, thermal resistance of adiabatic section is assumed to be negligible due to the small relative to the other resistances [6].

Table 3.1. THERMAL RESISTANCES ANALYSIS

Methods	Evaporator Section	Condenser Section
Method-1	$R_1 = \frac{\ln\left(d_{e,o}/d_{e,i}\right)}{2\pi\, k_{hp} L_e}$, $R_2 = \frac{\ln\left(d_{w,o}/d_{w,i}\right)}{2\pi\, k_{eff}\, L_e}$, $R_3 = \frac{1}{h_e \pi\, d_{e,i}\, L_e}$	$R_4 = \frac{1}{\pi\, d_{c,i} L_c h_c}$, $R_5 = \frac{\ln\left(d_{w,o}/d_{w,i}\right)}{2\pi\, k_{eff} L_c}$, $R_6 = \frac{\ln\left(d_{c,o}/d_{c,i}\right)}{2\pi\, k_{hp} L_c}$, $R_7 = \frac{t_{hp}}{\pi\, d_{c,o} L_c k_{hp}}$, $R_8 = \frac{1}{h_c \pi\, d_{c,o}\, L_c}$

Method-2	$R_1 = \frac{\sigma_m}{\pi k_{hp} d_m L_e}$, $R_2 = \frac{\sigma_m}{\pi k_{eff} d_m L_e}$, $R_3 = \frac{RT_s^2\sqrt{2\pi RT_s}}{\rho_v h_{fg}^2 \pi d_e L_e}$	$R_4 = \frac{RT_s^2\sqrt{2\pi RT_s}}{\rho_v h_{fg}^2 \pi d_c L_c}$, $R_5 = \frac{\sigma_m}{\pi k_{eff} d_m L_c}$, $R_6 = \frac{\sigma_m}{\pi k_{hp} d_m L_c}$, $R_8 = \frac{1}{\pi d_{c,o} L_c h_c}$
Method-3	$R_1 = \frac{\ln\left(d_{e,o}/d_{e,i}\right)}{2\pi k_{hp} L_e}$, $R_2 = \frac{\ln\left(d_{w,o}/d_{w,i}\right)}{2\pi k_{eff} L_e}$, $R_3 = \frac{1}{h_e \pi d_{e,i} L_e}$	$R_4 = \frac{1}{\pi d_{c,i} L_c h_c}$, $R_5 = \frac{\ln\left(d_{w,o}/d_{w,i}\right)}{2\pi k_{eff} L_c}$, $R_6 = \frac{\ln\left(d_{c,o}/d_{c,i}\right)}{2\pi k_{hp} L_c}$, $R_7 = \frac{\ln\left(d_{ma,o}/d_{ma,i}\right)}{2\pi k_{ma} L_{ma}}$

The total thermal resistance at the evaporator, condenser and condenser outlet of a wick heat pipe(ETC) can be written as:

$$R_t = R_1 + R_2 + R_3 + R_4 + R_5 + R_6 + R_7 + R_8 \quad (18)$$

The condenser outlet temperature of a wick heat pipe(ETC) can be expressed as the heat transfer rate between the wick heat pipe condenser outlet and ambient(or) inlet water.

$$Q = U_{hp,c} A_c \left(T_{c,o} - T_i\right) \quad (19)$$

4. RESULTS AND DISCUSSION:

4.1. Effective Monthly Solar Insolation and Condenser Outlet Temperature with the Best Collector Tilt Angles

Table 4.1 shows that the effective monthly solar insolation and condenser outlet temperature with the best collector tilt angles results on the collector's surface at 12:00 noon depend on YTU location. According to this result, solar insolation at 12:00 noon in March is higher than other months because the sun appears to be directly over the equator. In this case, the solar radiation is more intense in March(summer). Moreover, table 4.1 describes the monthly results at 12:00 noon of condenser outlet temperature of a wick heat pipe(ETC) by using Fluent software. According to the numerical results, wick heat pipe(ETC) can operate at horizontal position(0 degree) due to the pressure driving force from evaporator to condenser with wick effect. Furthermore, 0º to 40º numerical results indicate that a slight difference.

Table 4.1. EFFECTIVE MONTHLY SOLAR INSOLATION AND CONDENSER OUTLET TEMPERATURE

Months	The Best Collector Tilt Angles	Effective Solar Insolation(W/m^2)	Wick Heat Pipe Condenser Outlet Temperature(K)
January	35º	940.98	323.997
February	25º	960.76	323.995
March	15º	969.71	323.993
April	15º	969.09	323.992
May	0º	959.67	322.992
June	0º	943.69	321.992
July	0º	947.81	322.991
August	10º	956.58	322.993
September	15º	958	323.991
October	20º	954.91	323.994
November	35º	936.29	323.996
December	40º	921.23	323.998

4.2. Temperature Contours and Heat Transfer Process

The heat transfer process within a wick heat pipe(ETC) is investigated with the best collector tilt angles. Figure 3 shows that the heat transfer process of evaporator, adiabatic and condenser zones at 0º in May. According to these results, the surface wall temperature distribution in the evaporator is higher than the other zones due to the input solar heat flux(solar insolation). However, the condenser surface wall temperature is lower than the other zones that are heat energy is released. At the wall and liquid-wick regions, temperature distribution is a significantly change however at the vapor core region is a little change. Because wall and liquid-wick regions provide liquid combine wick with conjugate heat transfer effect but vapor only distribute at vapor core region.

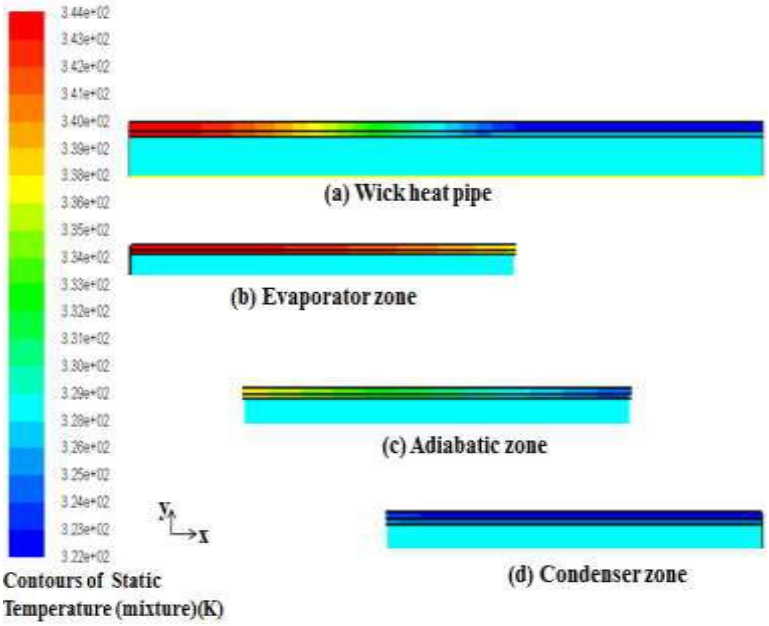

Fig. 3 Heat Transfer Process of a Wick Heat Pipe(ETC) in May, Tilt Angle(0 degree) at 60 min

4.3. Velocity Vector Distribution

Figure 4 shows that the velocity vector distribution of a wick heat pipe(ETC) at horizontal position. The velocity distribution results indicate that velocity vector direction along the vapor region has an ascending flow although this direction is a change downward flow for liquid-wick region of the wick heat pipe(ETC). According to this result, the velocity magnitude of adiabatic zone is higher than the other zones due to the transportation zone between evaporator and condenser.

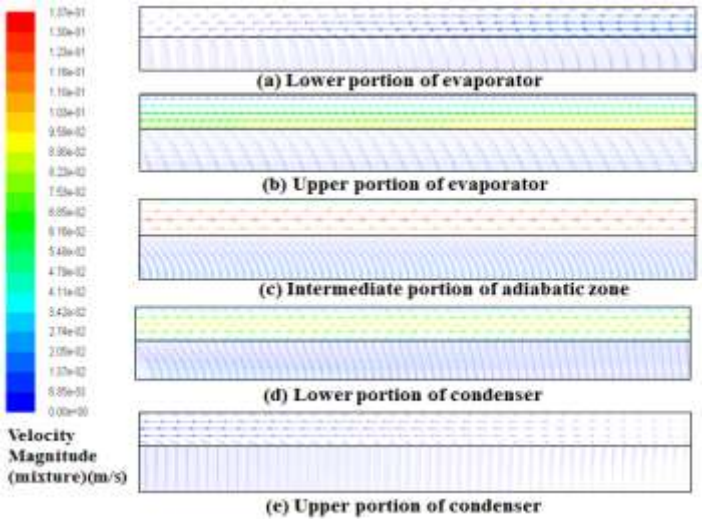

Fig. 4 Velocity Vector Distribution of a Wick Heat Pipe(ETC) in May, Tilt Angle (0 degree) at 60min

4.4. Comparing the Condenser Outlet Temperature between Numerical and Theoretical Results

Table 4.2 shows that the comparison between the numerical and theoretical(different three methods) condenser outlet temperature results of a wick heat pipe(ETC). It is seen that the theoretical result of Nagham Ismail's NTU method(method-1) is more agreement with numerical result of current model. Because this method considered conduction and convection thermal resistances at the condenser outlet to transfer of heat more detail.

Table 4.2. NUMERICAL AND THEORETICAL RESULTS

Numerical Results	Theoretical Results		
	Method-1	Method-2	Method-3
323.997	357.161	425.697	489.509
323.995	358.306	428.291	493.452
323.993	358.819	429.452	495.218
323.992	364.223	429.375	495.100
322.992	358.238	428.136	493.217
321.992	357.315	426.045	490.039
322.991	357.554	426.587	490.863
322.993	358.049	427.710	492.569
323.991	358.135	427.904	492.864
323.994	357.964	427.517	492.275
323.996	356.887	425.077	488.567
323.998	356.016	423.103	485.566

5. CONCLUSIONS:

In this paper, monthly solar insolation with the best collector tilt angles at 12:00 noon is determined on Insein, YTU. The surface wall temperature distribution of evaporator zone is higher than the other zones however; condenser zone is lower than the other zones. Because the latent heat energy is absorbed at the evaporator but latent heat energy is released at the condenser. The vapor and liquid flow distribution is investigated within a vapor and liquid-wick regions of a wick heat pipe(ETC) according to the capillary action. After that, velocity vector direction is observed with the two phase flow processes at the vapor and liquid-wick regions. According to the numerical and theoretical investigations, method-1 is more agreement with numerical results because this method considered solving heat transfer problem with complete thermal resistances of condenser outlet. Wick heat pipe(ETC) can be operated at horizontal position (tilt angle 0^o) and other angles for present research due to the capillary action and wick effect. Therefore, the numerical and theoretical investigations of heat transfer characteristics with wick heat pipe(ETC) model depend on horizontal and other inclination angles can be applied for solar water heating.

REFERENCES:

1. Hossein Abdi, (2012): “Evacuated tube solar heat pipe collector model and associated tests”, Journal of Renewable and Sustainable Energy 4, 023101-1-13.
2. Siva Kumar, (2017): “Experimental and theoretical investigation of evacuated tube solar collector with heat pipe”, International Journal of Innovative Research in Science, Engineering and Technology, Vol.6, Issue 3, pp.4050-4057.
3. Isam Janajreh, (2016): “Numerical simulation of a cylindrical heat pipe and performance study”, International Journal of thermal and environmental engineering, Vol.12, No.2, pp.135-141.
4. Shoeib Mahjoub, (2008): “Numerical simulation of a conventional heat pipe”, International Journal of Mechanical, Aerospace, Industrial, Mechatronic and Manufacturing Engineering, Vol.2, No.3.
5. Rakesh Hari, (2013): “Numerical analysis of two phase flow in flat heat pipe”, International Journal of Innovative Research in Science, Engineering and Technology, Vol.2, Special Issue 1.
6. Nagham Ismail, (2012). “Modeling of Solar Collector”. Final year project, Lebanese University, Faulty of Engineering III Mechanical Department.
7. ANSYS, ANSYS FLUENT User’s Guide, Release 15.0, ANSYS Inc., PA, USA, 2013.
8. Fluent, Fluent 6.3 UDF Manual, Fluent Inc., USA, 2006.
9. Fluent, Fluent 6.2 User’s Guide, Fluent Inc., USA, 2003.
10. John Wiley & Sons, (1981). “Fundamentals of Heat Transfer”, Canada.
11. http://www.westech.com/html/solar collector size.htm, installation manual.